J|A|C|S
ARTICLES
Published on Web 02/03/2006

In Silico Design of a Mutant of Cytochrome P450 Containing Selenocysteine

Shimrit Cohen, Devesh Kumar, and Sason Shaik*

Contribution from the Department of Organic Chemistry and the Lise Meitner-Minerva Center for Computational Quantum Chemistry, The Hebrew University, Jerusalem, 91904, Israel

Received September 26, 2005; E-mail: sason@yfaat.ch.huji.ac.il

Abstract: A mutant of $P450_{cam}$, in which the cysteine ligand was replaced by selenocysteine, was designed theoretically using hybrid QM/MM (quantum mechanical/molecular mechanical) calculations. The calculations of the active species, Se−CpdI (selenocysteine−Compound I), of the mutant enzyme indicate that *Se−Cpd I will be formed faster than the wild-type species and be consumed more slowly in C−H hydroxylation.* As such, our calculations suggest that Se−Cpd I can be observed unlike the elusive species of the wild-type enzyme (Denisov, I. G.; Makris, T. M.; Sligar, S. G.; Schlichting, I. *Chem. Rev.* **2005**, *105*, 2253−2277). Spectral features of Se−Cpd I were calculated and may assist such eventual characterization. The observation of Se−Cpd I will resolve the major puzzle in the catalytic cycle of a key enzyme in nature.

Introduction

Cytochrome P450 is an important metalloprotein enzyme that activates O_2 and performs vital transformations of organic molecules in all aerobic organisms including humans.[1,2] Despite this importance and the intensive investigations of the enzyme by scientists from a wide variety of different disciplines, the active species is unknown yet, and there is a real need for new isoforms or mutant enzymes, which can stabilize the active species or produce an improved function.[3−5] This Herculean effort by the experimental community[1−5] can be aided by theoretical design. Here we introduce a theoretically designed active species of a new mutant of P450 and argue that this mutant species, as opposed to the wild-type (WT) enzyme, is likely to be observable.

The putative active species is thought to be the Compound I (Cpd I) species,[6] in Figure 1A. A mutation that is likely to affect the electronic structure of the enzyme and the stability of the elusive[3,4] active species involves the replacement of the cysteine (SCys) residue, which creates the characteristic Fe−S bond of the enzyme,[7] by an Fe−Se bond[8] with the so-called 21st amino acid,[9] selenocysteine (SeCys), in Figure 1B. Since complexes with Fe−Se bonds have been prepared already,[8] it might be possible to generate the mutant selenocysteinato-P450, and this constitutes an incentive to try and predict the properties of the putative Se−Cpd I by theoretical means. As such, our theoretical work studies the electronic structure of this mutant species, its potential kinetic stability, characteristic spectroscopic param-

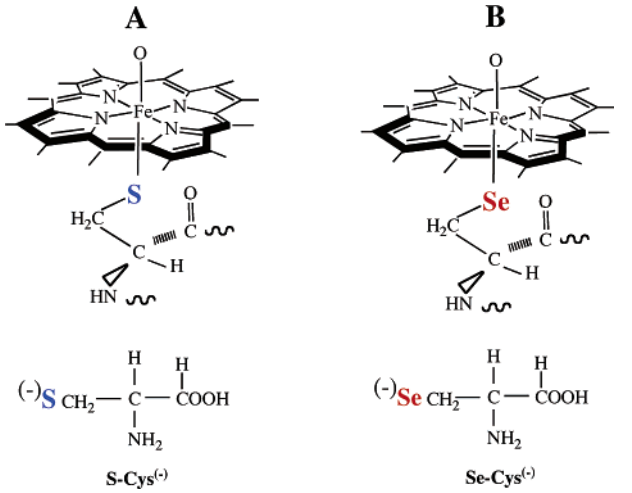

Figure 1. A schematic representation of the active species of P450, Compound I (Cpd I), showing only the iron-protoporphyrin IX unit and the two axial ligands, oxo and cysteinate (A). Part B shows the same species for a mutant in which cysteinate is replaced by selenocysteinate.

(1) Ortiz de Montellano, P. R., Ed. *Cytochrome P450: Structure, Mechanism and Biochemistry*, 3rd ed.; Kluwer-Academic/Plenum Press: New York, 2005.
(2) (a) Poulos, T. L.; Johnson, E. F. Chapter 3 (ref 1). (b) Guengerich, F. P. Chapter 10 (ref 1).
(3) Schlichting, I.; Berendzen, J.; Chu, K.; Stock, A. M.; Maves, S. A.; Benson, D. E.; Sweet, R. M.; Ringe, D.; Petsko G. A.; Sligar, S. G. *Science* **2000**, *287*, 1615−1622.
(4) Denisov, I. G.; Makris, T. M.; Sligar, S. G.; Schlichting, I. *Chem. Rev.* **2005**, *105*, 2253−2277.
(5) Yoshioka, S.; Takahashi, S.; Ishimori, K.; Morishima, I. *J. Inorg. Biochem.* **2000**, *81*, 141−151.
(6) Harris, D. L. *Curr. Opin. Chem. Biol.* **2001**, *5*, 724−735.
(7) Sono, M.; Roach, M. P.; Coulter, E. D.; Dawson, J. H. *Chem. Rev.* **1996**, *96*, 2841−2887.
(8) Quite a few complexes with Fe−Se bonds are known by now. For a selection of papers on these complexes, see: (a) Hauptmann, R.; Kliss, R.; Henkel, G. *Angew. Chem., Int. Ed.* **1999**, *38*, 377−379. (b) Song, L.-C.; Sun, Y.; Hu, Q.-M.; Liu, Y. *J. Organomet. Chem.* **2003**, *676*, 80−84. (c) Song, L.-C.; Yang, J.; Hu, Q.-M.; Wu, Q.-J. *Organometallics*, **2001**, *20*, 3293−3298. (d) Song, L.-C.; Fan, H.-T.; Hu, Q.-M.; Yang, Z.-Y.; Sun, Y.; Gong, F.-H. *Chem.—Eur. J.* **2003**, *9*, 170−180. (e) El-khateeb, M. *Inorg. Chim. Acta* **2004**, *357*, 4341−4344. (f) Short 1,3 distances between Fe and Se were observed in an iron coordinated with methylene groups: Mathur, P.; Manimaran, B.; Hossain, Md. M.; Rheingold, A. L.; Liable-Sands, L. M.; Yap, G. P. A. *J. Organomet. Chem.* **1997**, *540*, 165−168. (g) For a Se−Cys coordinated to Ni in the [NiFeSe] hydrogenase, see: Garcin, E.; Vernede, X.; Hatchikian, E. C.; Volbeda, A.; Frey, M.; Fontecilla-Camps, J. C. *Structure* **1999**, *7*, 557−566.
(9) (a) Chambers, I.; Frampton, J.; Goldfarb, P.; Affara, N.; McBain, W.; Harrison, P. R. *EMBO J.* **1986**, *5*, 1221−1227. (b) Zinoni, F.; Heider, J.; Böck, A. *Proc. Natl. Acad. Sci. U.S.A.* **1990**, *87*, 4660−4664.

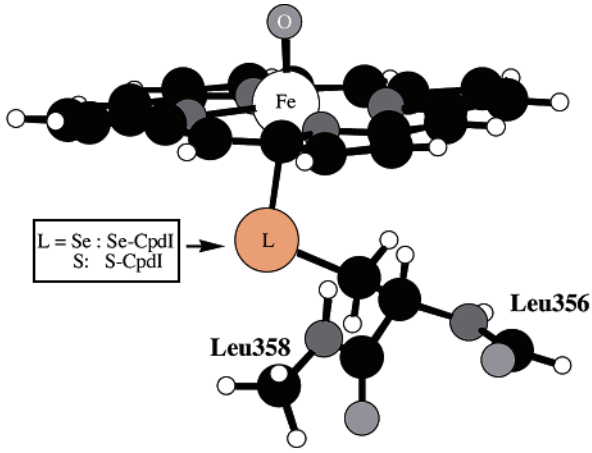

	Se-CpdI		S-CpdI
$^4A_{2u}[^2A_{2u}]$	Snapshot 1	Snapshot 2	Snapshot 2
r(Fe-O)	1.625 [1.626]	1.626 [1.626]	1.626 [1.625]
r(Fe-L)	2.779 [2.792]	2.727 [2.747]	2.555 [2.577]
r(Fe-N)	2.034 [2.034]	2.037 [2.038]	2.042 [2.038]
a(O-Fe-L)	172.4 [172.1]	171.3 [170.8]	172.9 [172.9]
a(Fe-L-C)	109.0 [108.8]	105.9 [105.5]	109.3 [109.1]

Figure 2. Key optimized (basis set B2) geometric parameters of Se−Cpd I in two snapshots and in the two lowest lying states. Snapshot 1 corresponds to 29 ps and snapshot 2 to 40 ps along the equilibrium trajectory (ref 10a). The two states are the quartet spin state, $^4A_{2u}$, and the doublet spin state, $^2A_{2u}$, which correspond to the ferromagnetic and antiferromagnetic coupling of the three unpaired electrons in Se−Cpd I. For comparison, we show alongside the optimized geometric parameters (basis set B2) of S−Cpd I in snapshot 2 for the $^4A_{2u}$ and $^2A_{2u}$ states.

eters, and C−H hydroxylation reactivity compared with the wild-type (WT) species. Its likelihood of being observed is a challenge to be followed by experiment.

Methods

Details of the various calculations are provided in the Supporting Information (SI); key results are discussed here. The preparation of the enzyme for QM/MM calculations and the molecular dynamic equilibration follows the detailed description in ref 10a. The following description focuses on the relevant details for the present study.

QM/MM Calculations. The selected QM region consists of 57 atoms and includes the oxo-iron-porphine, $SeCys_{357}$, CO group of Leu_{356}, and NH−C^{α}H unit of Leu_{358} (Figure 2). The total system consists of 24 395 atoms, including 16 956 solvent atoms. We applied the electronic embedding scheme[10b] as the QM/MM method. The complete nonbonding MM and QM/MM interactions were calculated without employing any cutoff. The hydrogen link atoms[10c] with the charge shift[10d] model were used to treat the QM/MM boundary. The QM/MM calculations were carried out with the ChemShell package,[11] which is interfaced with TURBOMOLE[12] that performs the QM calculations, and the CHARMM force field,[13] run through the DL-POLY program,[14a] which executes the MM calculations. Geometry optimizations were performed with the HDLC optimizer[14b] implemented in Chemshell.

The QM calculations employed the UB3LYP functional.[15] Two basis sets were used (see SI for more details), one consisting of an effective core potential coupled with a double-ζ quality (LACVP)[16a] on iron B1 and the other one being a larger basis set, B2, which involves a Wachters[16b] all electron basis set on iron and a 6-31+G* basis set on the atoms directly coordinated to iron; the rest of the atoms are described by the double-ζ basis set, 6-31G. For the Se−Cpd I calculations the Se atom is described by LACVP basis (B1) or LACVP+* basis (B2).

Spectroscopic parameters were calculated with program ORCA,[17] with the triply polarized core properties basis set CP(PPP) on iron[18] and the SV(P) basis set on all the rest of the atoms.[19]

Gas-Phase Calculations. Single-point gas-phase calculation were carried out at the geometry of the system in the enzyme environment and are referred to as $S_{p,g}$. Additional geometry optimizations on the QM regions, representing the active species, were performed in the gas phase in B1 and B2 basis sets and are referred to as $S_{g,g}$.

In addition, a model with small ligand (L) representations, L = SeH and SH, was used for the reactivity studies with a probe substrate that can undergo C−H hydroxylation. These calculations were done with B1, and a single-point energy evaluation was carried out with LACV3P+* (B2′), using JAGUAR 5.5.[20]

QM/MM Calculations of Se−Cpd I: The species of the selenocysteine-mutant, Se−Cpd I, were generated by replacing the cysteinate ligand ($SCys_{357}$ in $P450_{cam}$[21]) by selenocysteinate, followed by QM/MM geometry optimization. Our initial study of the doublet spin state for the resting state (the sixth ligand is H_2O) of the enzyme, using B1, revealed a normal heme complex with a Se−Fe bond of 2.47 Å (see Figure S21) that is very close to experimentally determined values of Fe−Se complexes (2.39−2.49 Å).[8] Following this, we chose for Se−Cpd I three snapshots (1, 2, and 3; corresponding to 29, 40, and 50 ps) from the equilibrium trajectory of the WT species.[10a] All these snapshots were optimized by QM/MM using the two basis sets B1 and B2. Since the essential differences are clear from snapshots 1 and 2, we display these two in the following text, while snapshot 3 is relegated to the SI (Figures S6 and S7). A molecular dynamics (MD) run of 200 ps on the optimized geometry of the Se−Cpd I species of snapshot 1 did not reveal any disruption of the protein structure of the mutant due to the "size" of selenium (see Figure S13 and S14, in the SI).

Results and Discussion

The optimized QM/MM geometric parameters of the Se−Cpd I species, for snapshots 1 and 2, at the highest level are shown in Figures 2 and 3, alongside the published[10a] theoretical results for the WT active species, S−Cpd I. The active species possesses three unpaired electrons;[6,10a] two are in a triplet configuration residing on the oxo-iron moiety, while the third is in an orbital of mixed nature of the porphyrin and the cysteinate or selenocysteinate ligands. As such, we show in Figures 2 and 3, for each snapshot, the key geometric features for the doublet and quartet states, which arise from the antiferromagnetic and ferromagnetic coupling modes between the triplet electrons in the FeO moiety and the third electron on

(10) (a) Schöneboom, J. C.; Lin, H.; Reuter, N.; Thiel, W.; Cohen, S.; Ogliaro F.; Shaik, S. *J. Am. Chem. Soc.* **2002**, *124*, 8142−8151. (b) Bakowies, D.; Thiel, W. *J. Phys. Chem.* **1996**, *100*, 10580−10594. (c) Antes, I.; Thiel, W. In *Hybrid Quantum Mechanical and Molecular Mechanical Methods*; Gao, J., Ed.; ACS Symposium Series 712; American Chemical Society: Washington, DC, 1998; pp 50−65. (d) de Vries, A. H.; Sherwood, P.; Collins, S. J.; Rigby, A. M.; Rigutto, M.; Kramer, G. J. *J. Phys. Chem. B* **1999**, *103*, 6133−6141.
(11) Sherwood, P. et al. *THEOCHEM* **2003**, *632*, 1−28.
(12) Ahlrichs, R. et al. *TURBOMOLE 5.5*; University of Karlsruhe: 2002.
(13) CHARMM22 force field: MacKerell, A. D., et al. *J. Phys. Chem. B* **1998**, *102*, 3586−3616.
(14) (a) Smith, W.; Forester, T. R. *J. Mol. Graph.* **1996**, *14*, 136−141. (b) Billeter, S. R.; Turner, A. J.; Thiel, W. *Phys. Chem. Chem. Phys.* **2000**, *2*, 2177−2186.
(15) Becke, A. D. *J. Chem. Phys.* **1993**, *98*, 5648−5852.
(16) (a) The LACVP family of basis sets, used in JAGUAR, is derived from LANL2DZ; see: Hay, J. P.; Wadt, W. R. *J. Chem. Phys.* **1985**, *82*, 299−310. (b) Wachters, A. J. H. *J. Chem. Phys.* **1970**, *52*, 1033−1036.
(17) Neese, F. *ORCA*-an ab initio, DFT and semiempirical electronic structure package, version 2.4, revision 10; Max-Planck-Institut für Strahlenchemie, Mülheim an der Ruhr: Germany, 2004.
(18) Neese, F. *Inorg. Chim. Acta* **2002**, *337*, 181−192.
(19) Schäfer, A.; Horn, H.; Ahlrichs, R. *J. Chem. Phys.* **1992**, *97*, 2571−2577.
(20) *JAGUAR 5.5*; Schrodinger, Inc.: Portland, OR.
(21) Mueller, E. J.; Lioda, P. J.; Sligar, S. G. Chapter 3 in *Cytochrome P450: Structure, Mechanism and Biochemistry*, 2nd ed.; Ortiz de Montellano, P. R., Ed; Plenum Press: New York, 1995.

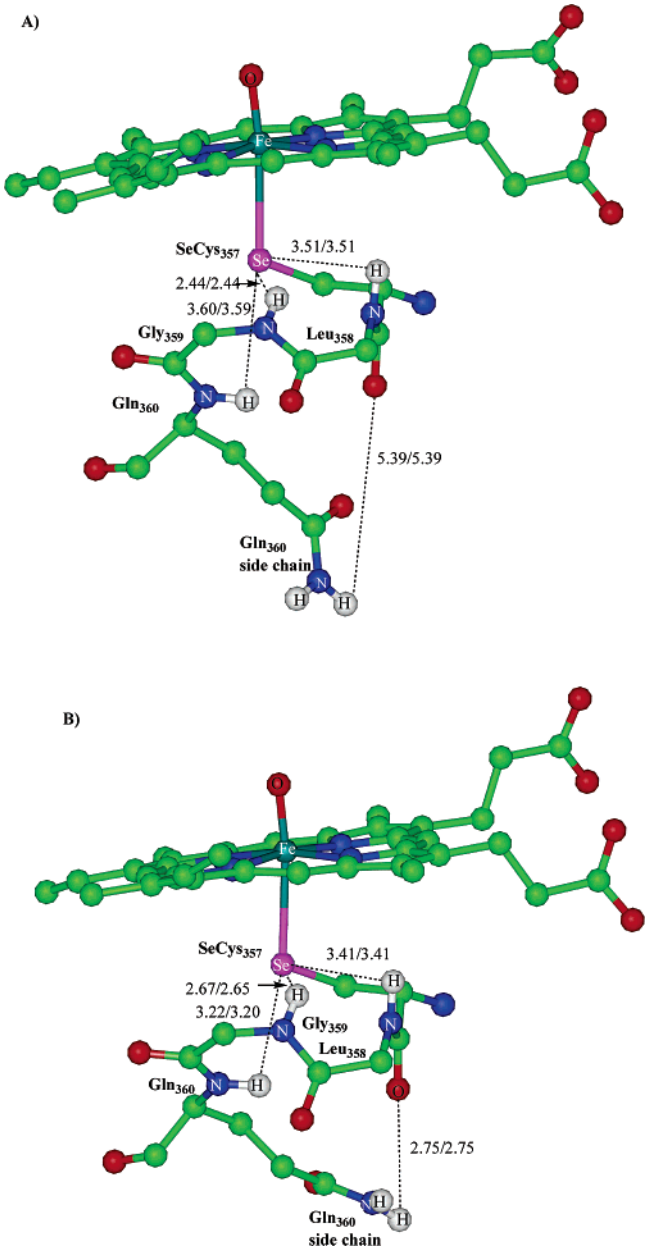

Figure 3. Hydrogen bonding-type interactions between the selenocysteine ligand ($SeCys_{357}$) and protein residues: Gln_{360}, Gly_{359}, and Leu_{358} in two snapshots; (A) snapshot 1 and (B) snapshot 2. The QM/MM optimized distances (basis set B2) are shown in the drawings. Note that the amidic hydrogen bond-type interaction, NH- - -O═C in part B, which is donated by the Gln_{360} side chain to the carbonyl group of Se−Cys_{357}, is detached in part A.

the porphyrin-(seleno)cysteine ligands. These states are commonly labeled as $^2A_{2u}$ and $^4A_{2u}$, respectively.[6,10a]

It is seen from Figure 2 that both Cpd I species possess a typically short Fe═O bond, ca. 1.63 Å.[3,6,10a] On the other hand, the Fe−Se bond is significantly longer than the Fe−S bond. Other key parameters are similar for the two species. The two snapshots shown in Figure 2 for Se−Cpd I are almost identical with the exception of the Fe−Se bond length, which is shorter for the structure in snapshot 2. Inspection of Figure 3A vs 3B shows that this bond shortening is associated with the NH- - -Se and the NH- - -O═C(SeCys) interactions[5,10a,22] among the

(22) Poulos, T. L. *J. Biol. Inorg. Chem.* **1996**, *1*, 356−359.

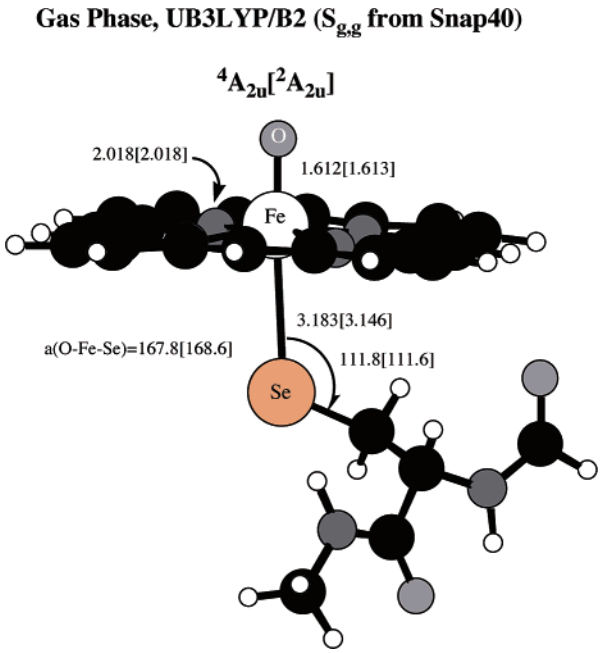

Figure 4. Optimized geometry (basis set B2) of Se−Cpd I for the two spin states $^4A_{2u}$ and $^2A_{2u}$ in gas-phase conditions (labeled as $S_{g,g}$).

residues Gln_{360}, Gly_{359}, and Leu_{358} and the selenium and carbonyl oxygen atoms of Se−Cys_{357}. Note that these are not classical hydrogen bonds in the structural sense (the N−H−Se angles are not linear), and therefore we refer to them as hydrogen bonding-type interactions. These interactions were shown to affect the properties of the WT enzyme, including its reactivity toward oxidizable substrates.[5] As in the case of the WT species,[10a] here too the NH- - -SeCys distances of the two snapshots differ mostly in the distance of the interaction of the Gln_{360} side chain with the carbonyl group of the selenocysteine ligand; this distance is shorter for snapshot 2 (2.75 vs 5.39 Å) where also the Fe−Se bond is shorter (2.727 Å vs 2.779 Å).

The impact of the protein becomes more apparent by looking at the Se−Cpd I in the gas phase, without any external interactions, as shown in Figure 4. It is seen that the gas-phase species possesses a shorter Fe═O bond and a long Fe−Se distance of 3.18 Å (for $^4A_{2u}$). Changing the ligand representation to a maximally truncated model, HSe^-, leads to the same outcome, namely, a long Fe−Se bond of ca. 2.99 Å (see Figures S8 and S15 in the SI). In fact, in the gas phase the Fe−Se bond is virtually "dissociated" to a selenocysteinyl radical and a reduced pentacoordinated Cpd I species. Thus, the protein exerts a dramatic effect and is responsible for the stability of the Se−Cpd I species, more so than in the case of the WT S−Cpd I species, where the bond length changes from 2.68 to 2.70 Å in the gas phase to 2.56−2.58 Å in the protein.[10a]

The protein exerts its effect on the active species via two factors; one is electronic, and the other is a steric restraint. Figure 5 shows the energetic contributions of the two factors, using the Se−Cpd I species in the protein ($S_{p,p}$), in the gas phase with optimized geometry ($S_{g,g}$), and in the gas phase with the frozen geometry as in the protein ($S_{p,g}$). It is seen that relative to the bare species $S_{p,g}$, the protein stabilizes Se−Cpd I ($S_{p,p}$) by a significant amount (ΔE_{vert}), 142.3/142.4 kcal/mol for $^4A_{2u}/^2A_{2u}$ respectively. This stabilization corresponds to the interactions of the active species with the electric field of the protein and its hydrogen bonding donors. Some of these interactions, which

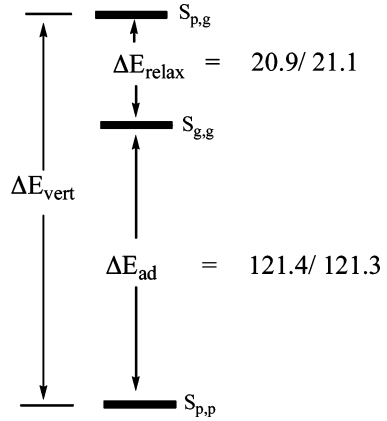

Figure 5. Relative energies (kcal/mol) for Se−Cpd I in three situations: $S_{g,g}$ corresponds to the species in the relaxed gas-phase geometry and in gas-phase conditions (no interactions), $S_{p,g}$ corresponds to the species with the geometry frozen as in the protein but in gas-phase conditions, and finally, $S_{p,p}$ corresponds to the species within the protein environment and in the relaxed geometry within the protein. ΔE_{vert} corresponds to the vertical stabilization energy of Se−Cpd I by the protein at the geometry within the protein, ΔE_{relax} corresponds to the energy change due to the geometry relaxation of the gas-phase species, and ΔE_{ad} is the adiabatic stabilization energy. The relative energy values separated by a slash refer to the two spin states $^4A_{2u}/^2A_{2u}$ respectively.

Table 1. Spin Densities and Charges, B2 Basis Set

	spin, $^4A_{2u}$			charge, $^4A_{2u}$		
Se–Cpdl system	ρ_{FeO}	ρ_{por}	ρ_{SeCys}	Q_{FeO}	Q_{por}	Q_{SeCys}
$S_{g,g}$	1.999	0.177	0.825	0.992	−0.787	−0.205
$S_{p,p}$(Snap2)	1.999	0.601	0.400	1.136	−0.599	−0.537
$S_{p,p}$(Snap1)	1.988	0.547	0.466	1.134	−0.635	−0.499
S–Cpdl system[a]	ρ_{FeO}	ρ_{por}	ρ_{SCys}	Q_{FeO}	Q_{por}	Q_{SCys}
$S_{g,g}$	2.015	0.457	0.528	0.961	−0.693	−0.268
$S_{p,p}$(Snap2)	2.015	0.734	0.251	0.980	−0.469	−0.511

[a] Recalculated here with B2.

are directed at the selenium, were shown above in Figure 3; their impact can be appreciated from the fact that in snapshot 2 the Fe−Se bond length gets a bit shorter, as the distance Gln_{360}NH- - -O=C($SeCys_{357}$), between the Gln_{360} side-chain and $SeCys_{357}$, decreases compared with snapshot 1. Similarly, in snapshot 3 (Figures S6, S7 and Table S9) the lengthening of the Leu_{358}NH- - -Se distance and the rather long Gln_{360}NH- - -O=C($SeCys_{357}$) distance cause a slight elongation of the Fe−Se bond, compared with snapshot 2. Thus, the NH- - -O=C($SeCys_{357}$) and NH- - -$SeCys_{357}$ interactions of the three amino acid residues with the SeCys ligand contribute to the stabilization of a short Fe−Se bond in the mutant.

The second quantity in Figure 5 is the energy change between the optimized ($S_{g,g}$) and frozen gas phase ($S_{p,g}$) species, ΔE_{relax}. This quantity shows the amount of strain that has to be expended by the protein to clamp the active species and change its Fe−Se bond from the relaxed gas-phase value to the value in the protein. The values of ΔE_{relax}, ca. 21 kcal/mol, are rather similar to those of the WT S−Cpd I species,[10a] showing that there is no unusual strain in the Se−Cpd I species; in both cases the strain energy is significant but is overcompensated by the electrostatic effects (ΔE_{vert}) described above. The net stabilization is ΔE_{ad}, in Figure 5.

The data in Table 1 show the impact of electrostatic factors on the spin density (ρ) distribution in the active species in the $^4A_{2u}$ state (the $^2A_{2u}$ state has very similar values, Tables S6−S8). Thus, the Fe=O moiety carries a spin density of ∼2.0, in accord with the presence of two electrons in a triplet configuration on this moiety.[6,10a] However, the third spin is distributed in a manner dependent on the conditions: In the relaxed gas-phase geometry ($S_{g,g}$) the SeCys ligand is virtually a radical, with 82.5% of the spin density of the third unpaired electron residing on the selenium and only 17.7% on the porphyrin. By contrast, inside the protein ($S_{p,p}$), the spin on the SeCys ligand is reduced to 40−47%. At the same time, the porphyrin ligand of Se−Cpd I gains spin density, which increases from 17.7% to 55−60%. These trends are reflected also in the charges (Q) of the groups; in the gas phase, the SeCys ligand has a small negative charge, −0.205, being almost a radical species, whereas inside the protein the negative charge on the ligand is doubled, −(0.50−0.54). It follows therefore that, in the gas phase, the selenocysteinate anion is a good electron donor that transfers almost a full electron to the oxo-iron porphyrin moiety. Inside the protein environment the anionic form, selenocysteinate, is somewhat stabilized, resulting thereby in reduced charge transfer to the oxo-iron porphyrin. Similar trends were reported for the WT species; the spin density on the cysteine ligand is reduced from 53% in the gas phase to a small value of 25.1% in the protein pocket.[10a] Thus, while both ligands push electron density to the oxo-iron porphyrin, *the selenocysteine in the Se−Cpd I mutant relays significantly more electron density compared with the cysteine in the WT S−Cpd I.*

The ability of the axial ligand to donate electrons (known also as the "push effect"[7]) to the iron-porphyrin has been identified as a crucial factor for the O−O bond cleavage and the formation of Cpd I from the precursor ferric hydroperoxide species ($FeOOH^-$).[4,7,21,23] As shown by recent computational evidence,[24a] the electron releasing property of cysteinate facilitates the heterolytic cleavage (to Cpd I plus OH^- that gets protonated[24b]) process by as much as 81 kcal/mol. The results in the present paper show that selenocysteine will have an even larger "push effect". Since all the features that are required to facilitate the formation of Cpd I (higher basicity of $FeOOH^-$ and easier heterolytic O−O cleavage[24a,b]) are improved by selenium, we expect that Se−Cpd I should be formed faster than S−Cpd I from the respective ferric hydroperoxide species. In fact, the same "push effect" will very likely make Se−Cpd I less electrophilic by releasing electron density toward the high-valent oxo-iron moiety. As such, we may expect Se−Cpd I to be somewhat less reactive than S−Cpd I.

To gauge the relative reactivity of Se−Cpd I and S−Cpd I, we computed the barriers for C−H hydroxylation from a reactive substrate *trans*-2-phenyl methylcyclopropane.[25] For Se−Cpd I, the lowest computed and zero-point energy corrected barrier, for the reaction nascent from the $^2A_{2u}$ state, is 15.6 kcal/mol, i.e., 1.6 kcal/mol larger than the previously calculated[26] barrier,

(23) Kaizer, J.; Costas, M.; Que, L., Jr. *Angew. Chem., Int. Ed.* **2003**, *42*, 3671−3673.
(24) (a) For a recent gauging of the "push effect" by computational means, see: Ogliaro, F.; de Visser, S. P.; Shaik, S. *J. Inorg. Biochem.* **2002**, *91*, 554−567. Ogliaro, F.; de Visser, S. P.; Cohen, S.; Sharma, P. K.; Shaik, S. *J. Am. Chem. Soc.* **2002**, *124*, 2806−2817. (b) For a recent study of generating S−Cpd I from the $FeOOH^-$ precursor, showing a significant barrier for protonation, see: Kumar, D.; Hirao, H.; de Visser, S. P.; Zheng, J.; Wang, D.; Thiel, W.; Shaik, S. *J. Phys. Chem. B* **2005**, *109*, 19946−19951.
(25) Newcomb, M.; Toy, P. H. *Acc. Chem. Res.* **2000**, *33*, 449−455.
(26) Kumar, D.; de Visser, S. P.; Sharma, P. K.; Cohen, S.; Shaik, S. *J. Am. Chem. Soc.* **2004**, *126*, 1907−1920.

Table 2. Mössbauer Spectroscopic Parameters for Se−Cpd I and S−Cpd I of $P450_{cam}$[a]

	Se−CpdI		S−CpdI[b]
$^4A_{2u}/^2A_{2u}$	snapshot 1	snapshot 2	snapshot 2 [gas phase]
δ (mm/s)	0.11/0.11	0.12/0.12	0.13/0.13 [0.09/0.09]
ΔEq (mm/s)	1.21/1.19	0.99/1.00	0.64/0.67 [1.33/1.34]
η	0.07/0.08	0.02/0.02	0.10/0.09 [0.03/0.06]
J[c] (cm^{-1})	−24.6	−22.8	−16 [−27]

[a] Computed from single-point calculations at the B3LYP/CHRMM22 level with iron CP(PPP) and decontracted SV(P) basis set. [b] Values are taken from ref 27. [c] $\hat{H} = -2J\hat{S}_A \cdot \hat{S}_B$. J is obtained from the formula $J = (E_Q - E_D)/(\langle S^2\rangle_Q - \langle S^2\rangle_D)$, where Q is the quartet state, $^4A_{2u}$, and D the doublet $^2A_{2u}$ state. See ref 18 for details. $E_Q - E_D = 45.5/49.0\ cm^{-1}$ (for snaposhots 1/2).

14.0 kcal/mol, for the corresponding state of S−Cpd I (see Figure S18 and Table S12). Inclusion of environmental effects[26] that mimic the protein environment, i.e., NH- - -Se(S) interactions and the effects of bulk polarity, using a dielectric medium with a dielectric constant of 5.71 (and a probe radius of 2.72 Å), increase the difference to 2.7 kcal/mol, while single-point calculations with the larger basis set, LACV3P$^+$*, have a small effect in the same direction, making the barrier higher by 3.2 kcal/mol. As such, due to the increasing electron releasing property of selenium, Se−Cpd I is likely to be generated faster than S−Cpd I and to be consumed somewhat slower (approximately 100 times if we use the 2.7−3.2 kcal/mol difference in the barriers for the low-spin reaction; see Table S12) in the presence of a substrate that can undergo only C−H hydroxylation. This increases the chances that, unlike the elusive S−Cpd I,[4] the mutant Se−Cpd I may be an observable species.

For eventual identification of Se−Cpd I, we show in Table 2 Mössbauer parameters for Se−Cpd I alongside the values computed for the WT species.[27] Tabulated are the isomer shift, $\delta(^{57}Fe)$, the quadrupole splitting, ΔE_Q, and the asymmetry parameter, η. It is seen that the ΔE_Q and η parameters of Se−Cpd I are significantly different than those for S−Cpd I and are in fact more similar to the gas-phase values for the latter species.[27] Thus, once again we see the fingerprints of the "push effect";[7] these spectroscopic parameters reflect the greater donation of electron density from the SeCys ligand, which renders the Se−Cpd I species somewhat similar to the gas-phase species of the WT S−Cpd I.

The exchange coupling constant, J (Table 2), is a measure of the interaction energy between the spins on the Fe═O moiety and the spin on the porphyrin-SeCys/SCys ligand, in an a_{2u} orbital.[6,10a,27−30] The negative J means that the interaction is antiferromagnetic and stabilizes the doublet state below the quartet state. It is seen that the S−Cpd I exhibits the same type of coupling, albeit slightly smaller; here too the increased "push effect" of Se makes the spectroscopic parameter for Se−Cpd I closer to the gas-phase parameter of S−Cpd I.[27] The antiferromagnetic coupling in Se−Cpd I is of the same order of magnitude as that in the observable S−Cpd I species of the enzyme chloroperoxidase (CPO).[29] By contrast, all known synthetic Cpd I species have ferromagnetic coupling.[6,28] It was argued[28,30] that the negative J value of S−Cpd I of CPO indicates that the a_{2u} orbital is delocalized. Indeed, the extent of delocalization in Se−Cpd I is significant as may be deduced from the fact that the spin density on SeCys and porphyrin in Se−Cpd I is almost 50:50 in the protein (Table 1). Thus, the enhanced "push effect" of the SeCys is reflected also in the values of the exchange coupling constant parameter.

Finally, electronic spectroscopy has been used as a marker for S−Cpd I in, e.g., CPO.[6,31] For the WT S−Cpd I our computational values (TDDFT) show a Soret band with two maxima at 320−340 nm and a more distant one at 390 nm and a Q-band with two weak broad maxima at 550−645 nm; as in other theoretical results, here too[6,32] both bands are slightly red-shifted (by 30−50 nm) relative to the experimental values. The corresponding computed values for Se−Cpd I are different; the Soret band has two maxima with almost equal intensity at 313−318 and 333−336 nm, while the Q-band exhibits two low intensity absorptions clustered around 557−559 and 642−646 nm.

Conclusions

In sum, the in silico designed Se−Cpd I species of $P450_{cam}$ is similar to the WT species.[10a] However, the greater electron donation ability ("push effect"[7]) of the so-called 21st amino acid, selenocysteine compared with cysteine, suggests that the corresponding Se−Cpd I species will be formed faster, and since the study shows also a less reactive species toward C−H hydroxylation, we conclude that Se−Cpd I has more chances of being observed, compared with the WT S−Cpd I species. Its observation will solve one of the remaining big puzzles in the catalytic cycle of this enzyme.

Acknowledgment. The research was supported in parts by the German Federal Ministry of Education and Research (BMBF) within the framework of the German-Israeli Project Cooperation (DIP) and the Israel Science Foundation (ISF).

Supporting Information Available: References 11−13 in full, 14 tables, and 21 figures with structures and profiles (PDF). This material is available free of charge via the Internet at http://pubs.acs.org.

JA056586C

(27) Schöneboom, J. C.; Neese, F.; Thiel, W. *J. Am. Chem. Soc.* **2005**, *127*, 5840−5853.
(28) Weiss, R.; Mandon, D.; Wolter, T.; Trautwein, A. X.; Müther, M.; Bill, E.; Gold, A.; Jayaraj, K.; Terner, J. *J. Bioinorg. Chem.* **1996**, *1*, 377−383.
(29) Rutter, R.; Hager, L. P.; Dhonau, H.; Hendrich, M.; Valentine, M.; Debrunner, P. *Biochemistry* **1984**, *23*, 6809−6816.
(30) (a) Green, M. T. *J. Am. Chem. Soc.* **2001**, *123*, 9218−9219. (b) Green, M. T.; Dawson, J. H.; Gray, H. B. *Science* **2004**, *304*, 1653−1656.
(31) Egawa, T.; Proshlyakov, D. A.; Miki, H.; Makino, R.; Ogura, T.; Kitagawa, T.; Ishimura, Y. *J. Biol. Inorg. Chem.* **2001**, *6*, 46−54.
(32) Harris, D.; Loew, G.; Waskell, L. *J. Inorg. Biochem.* **2001**, *83*, 309−318.